LA-UR-03-1468

Application of Frequency Domain ARX Models and Extreme Value Statistics to Damage Detection

Timothy R. Fasel, Hoon Sohn and Charles R. Farrar

Engineering Sciences & Applications Division, Weapon Response Group, M/S T006
Los Alamos National Laboratory, Los Alamos, NM 87545

ABSTRACT

In this study, the applicability of an auto-regressive model with exogenous inputs (ARX) in the frequency domain to structural health monitoring (SHM) is explored. Damage sensitive features that explicitly consider the nonlinear system input/output relationships produced by damage are extracted from the ARX model. Furthermore, because of the non-Gaussian nature of the extracted features, Extreme Value Statistics (EVS) is employed to develop a robust damage classifier. EVS is useful in this case because the data of interest are in the tails (extremes) of the damage sensitive feature distribution. The suitability of the ARX model, combined with EVS, to nonlinear damage detection is demonstrated using vibration data obtained from a laboratory experiment of a three-story building model. It is found that the current method, while able to discern when damage is present in the structure, is unable to localize the damage to a particular joint. An impedance-based method using piezoelectric (PZT) material as both an actuator and a sensor is then proposed as a possible solution to the problem of damage localization.

1. INTRODUCTION

Many aerospace, civil and mechanical systems continue to be used despite aging and the potential for damage accumulation and unpredicted failure. If a damage detection method based on measured vibration response can be developed, it would constitute a more economical and quantifiable damage detection method than is currently available. Such a damage identification scheme can potentially provide significant economic and life-safety benefits by preventing unforeseen catastrophic failures. There are currently many nondestructive evaluation (NDE) methods for identifying damage in structures. However, current NDE methods are costly visual procedures or localized experimental methods such as acoustic or ultrasonic methods, magnetic field methods, radiograph, eddy-current methods and thermal field methods. These approaches are limited in usage, as the vicinity of the damage must be known *a priori* and easily accessible. For a more complete literature review of current SHM methods, consult Doebling et al., 1998. Many previous studies in the literature review focus on predicting damage using linear characteristics. Because damage to a structure will almost certainly result in some nonlinear behavior, a damage detection scheme that seeks to use nonlinear characteristics to identify damage could be of great use.

The focus of this study is to demonstrate the feasibility of a vibration-based damage detection system, using nonlinear data characteristics, for mechanical structures. In recent years, vibration-based damage detection techniques have come to the foreground as a legitimate method to determine structural damage. Many techniques have been investigated in this area. However, none has worked well enough to be considered for use in real world applications. Most techniques have problems being applied to various structures and the analysis of vibration data received can be a time intensive process. This study will attempt to investigate a damage detection technique that has not been extensively explored. This approach uses ARX frequency domain model coefficients originally proposed by Adams and Allemang [2] as the damage sensitive features. These features are then analyzed using a statistical method known as EVS. The approach taken in this study is unique in that it uses nonlinear analysis, as opposed to the linear techniques currently employed, to identify damage within the structure.

2. EXPERIMENTAL SETUP

The test structure shown in Figures 1 and 2 is a simulated three-story frame structure, constructed of unistrut columns and aluminum floor plates. Floors were 0.5-in-thick (1.3-cm-thick) aluminum plates with two-bolt connections to brackets on the unistrut columns. Floor heights were adjustable. The base was a 1.5-in-thick (3.8-cm-thick) aluminum plate. Support brackets for the columns were bolted to this plate. All bolted connections were tightened to a torque of 220 inch-pounds (25 Nm) in the undamaged state. Four Firestone airmount isolators, which allowed the structure to move freely in horizontal directions, were bolted to the bottom of the base plate. The isolators were mounted on aluminum blocks and plywood so that the base of the structure was level with the shaker. The isolators were inflated to 10 psig (69 kPag). The shaker was connected to the structure by a 6-in-long (15-cm-long), 0.375-in-dia (9.5-mm-dia) stinger connected to a tapped hole at the mid-height of the base plate. The shaker was attached 3.75-in (9.5-cm) from the corner on the 24-in (61-cm) side of the structure, so that both translational and torsional motion would be excited.

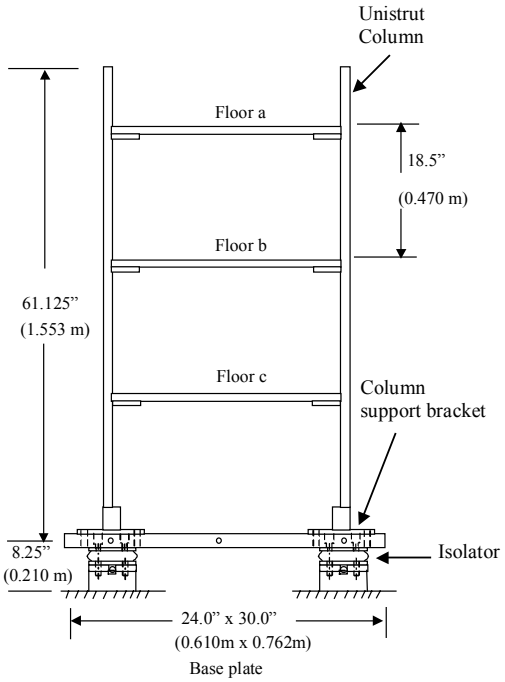

Figure 1: A side view of the assembled test structure

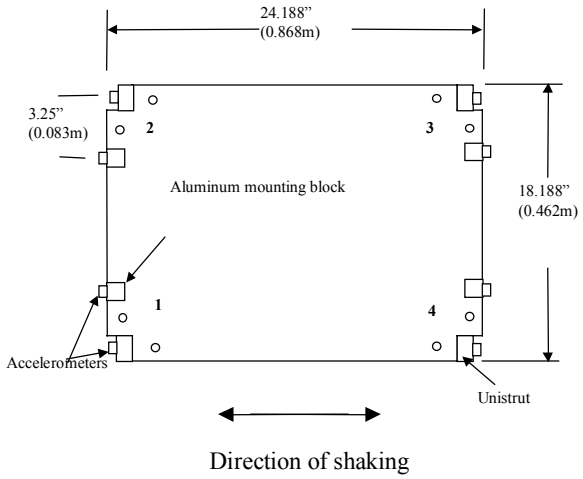

Figure 2: A top view of the assembled test structure

In this experiment, damage is simulated in joints through the loosening of the preload applied by the bolts at the joints of the structure. A "healthy" joint is held together by bolts that are torqued to a value of 220 inch-pounds (25 Nm). Multiple damage levels are then used so that the sensitivity of the damage detection method can be tested. The first damage level is simulated by loosening the preload on the bolts at the selected damaged joint to 15 inch-pounds (1.8 Nm). The next level has the preload being loosened to 5 inch-pounds (0.6 Nm). Bolts on the selected joint are then completely removed to simulate a crack in the joint for the final damage level. An electro-dynamic shaker attached to the base of the structure applies vibration input. The input excitation is a random waveform with a uniform energy content at the frequency range of 0 to 200 Hz. Two different base excitation levels were used in the experiment by changing the voltage supplied to the amplifier that powered the shaker. The root mean square (RMS) value of the high excitation level was 1 V, and that of the low excitation level was 0.25 V.

The structure is instrumented with 24 piezoelectric accelerometers. 2 accelerometers were placed at each joint with one accelerometer attached to the plate and the other accelerometer attached to the unistrut column (Figure 2). Each accelerometer was labeled with its own corresponding channel in the data acquisition system. Joints were labeled according to their locations on the floor and corner of the structure. Each corner was given a number (1-4) and each floor was given a letter (a-c) with (a) being the top floor of the structure and (c) the first floor. This labeling system is illustrated in Figures 1 and 2. Accelerometers are mounted on blocks glued to the floors and unistrut columns. This configuration allows relative

motion between the column and the floor to be detected. The nominal sensitivity of each accelerometer is 1 V/g. A commercial data acquisition system controlled from a laptop PC is used to digitize the accelerometer and force transducer analog signals.

For this study, 8-second time histories were sampled at a rate of 512 Hz, producing 4096 time points. A matrix of baseline undamaged data sets were recorded before damage was introduced to the structure. To test the robustness of the proposed method, different joints, along with multiple joints, were damaged as shown in Table 1. For each damage case and base excitation level, three separate time histories were recorded. Before acquiring each data set, the pressure in the air mounts was inspected, the bolt torques throughout the structure were verified and the accelerometers were inspected for proper mounting.

Table 1: Summary of damage cases

Damage Case 1	Joint 2a has induced damage
Damage Case 2	Joint 4b has induced damage
Damage Case 3	Joints 2a and 4b have induced damage

3. STRUCTURAL HEALTH MONITORING

The aforementioned test structure is analyzed using a damage detection process that is the focus of this study. SHM consists of the following four-part processes based on a statistical pattern recognition paradigm (Farrar et al., 2001).

3.1 Operational Evaluation

Operational evaluation determines the conditions under which the system to be monitored functions. The first step in this assessment is to define and, to the extent possible, quantify the damage that is to be detected. Limitations on data able to be retrieved for the damage detection process are also strictly defined during this stage. Because the test structure is located in a controlled laboratory environment, many of the evaluation problems that plague real world applications are not present. For instance, many real world structures are too large to be sufficiently excited using a shaker or impact hammer. In these cases, only ambient background vibration can be used to evaluate the condition of the building, which substantially hampers the potential effectiveness of SHM methods. Ambient vibration is typically nonstationary and produces a low frequency response that is insensitive to local damage.

In this study, varying levels of shaker input were used to introduce operational and environmental variability. The damage detection scheme should be insensitive to excitation level. This insensitivity to excitation level is often accomplished through a data normalization procedure.

3.2 Data Acquisition

Data acquisition in a SHM process begins with the selection of the types of sensors to be used, placement of the sensors, the number of sensors to be used, and the hardware used to transmit the data from the sensors into storage. Intervals at which data are taken must be explored, as the amount of data necessary depends on the specific structure as well as the type of damage to be detected.

3.3 Feature Extraction

Feature selection involves the extraction of certain kinds of information from the data that allow a distinction to be made between a damaged and an undamaged structure. This selection involves the condensation of the large amount of available data into a much smaller data set that can be analyzed in a statistical manner. Most of the articles in the technical journals focus on this aspect of SHM. Previous studies focus on extracting linear features for damage detection.

The features that are analyzed in this study are drawn from frequency domain analysis of the time histories obtained during experimentation on the test structure. Frequency response is important in structural dynamics because it relates inputs and outputs of the structure at various frequencies. Analyzing these responses can lead to helpful information regarding the

health of the structure. Conventional frequency response function estimators are based on a linearity assumption of the system. Though many large buildings can be approximated as behaving in a linear fashion, there are always local nonlinearities within the structures. Damage to a joint in a building will almost certainly be nonlinear in nature, and any method that seeks to identify damage location and severity will be enhanced by taking into account this nonlinear behavior. To take into account this nonlinearity, an ARX model is fitted to a frequency domain transmissibility. In a traditional time-series frame, an ARX model attempts to predict output at the current time point based on its own past time point outputs, as well as the current and past inputs to the system. A frequency domain ARX model attempts to predict the output at a particular frequency based on the input at that frequency, as well as outputs at surrounding frequencies. The outputs at the surrounding frequencies are included as the inputs to the model to account for subharmonics and superharmonics introduced to a system through a nonlinear feedback. Therefore, the features to be examined in this study are the exogenous and auto-regressive model coefficients in a frequency domain transmissibility model.

There are many possible forms of the frequency domain ARX model, with each depending on how many subharmonics and superharmonics are to be considered. In this case, a first order model is used to account for the effects of nonlinearities in the system. This ARX model in the frequency domain is as follows:

$$Y(k) = B(k)U(k) + A_1(k)Y(k - 1) + A_{-1}(k)Y(k + 1) \quad \textbf{(1)}$$

where $Y(k)$ is the response at *kth* frequency, $U(k)$ is the input at *kth* frequency, and $Y(k-1)$ and $Y(k+1)$ are the responses at *(k-1)th* and *(k+1)th* frequencies, respectively. $A_1(k)$ and $A_{-1}(k)$ are the frequency domain auto-regressive coefficients, and $B(k)$ is the exogenous coefficient. In this study, Equation (1) is used to predict what the frequency response of one accelerometer will be given the frequency response of the second accelerometer as well as the frequency response of the harmonics of the first accelerometer. That is, one accelerometer response is treated as an input and the other accelerometer response is treated as an output. The features to be examined in this study are the exogenous and auto-regressive model coefficients in a frequency domain transmissibility model. The differentiation of these two features is important: While the exogenous coefficients describe the linear transmissibility effects, the auto-regressive coefficients describe any nonlinear effects that may be present in the system. These coefficients are used as features to differentiate between damaged and non-damaged cases. More details on frequency domain analysis of data using an auto-regressive exogenous (ARX) input model can be found in Adams and Allemang, 2000, and Adams, 2001. Because $Y(k)$ and $U(k)$ in Equation (1) are complex numbers, the $B(k)$, $A_1(k)$ and $A_{-1}(k)$ coefficients also become complex. This means that for each frequency k, there are 6 unknown coefficients that must be determined.

In order to determine the ARX coefficients, multiple sets of data need to be taken while the structure is in the same condition. All time history data are first normalized by subtracting the mean and dividing by the standard deviation. This step helps the process be less sensitive to sources of variability, such as base excitation levels, introduced during testing. Because only three 4096-point time histories are available for each damage condition, each time history is split up into five separate 2048-point blocks, with 75% overlap. A FFT is then applied to each block of data in order to transfer the time history information into the frequency domain.

Now, there are 15 FFTs (5 from each of the available three time histories) and 6 unknown coefficients for each damage condition that must be solved. $B(k)$, $A_1(k)$ and $A_{-1}(k)$ are then determined by solving an overdetermined least-squares problem for every frequency k. Coefficients for the undamaged baseline condition are determined using only two of the available three time signals. This means that the 6 unknown coefficients are calculated using only 10 FFTs. This calculation is repeated three times using different combinations of two signals out of the three time signals. The combinations used in these three cases are the first and second, second and third, and first and third signals. This procedure is necessary because damage is diagnosed through examination of differences in coefficients between the undamaged state and the damaged state, and the decision boundary for the coefficient difference needs to be established from the undamaged condition. Therefore, the threshold values for damage classification are set up using the two sets of the baseline ARX coefficients, and the third set of undamaged coefficients is used for a false positive test.

3.4 Statistical Model Development

Statistical model development is the area of SHM that is least developed to date. Very few of the available SHM techniques have incorporated an algorithm that analyzes the extracted features from the data and unambiguously determines the damage state of the structure. Examination of the aforementioned features using rigorous statistical procedures should yield information that allows a diagnosis of damage state in the structure being monitored.

Because the information being sought is a measure of the nonlinearity of the data, the auto-regressive coefficients are used instead of the exogenous coefficients for analysis of the results. Because of the symmetry in the ARX frequency domain model, it is not necessary to analyze both auto-regressive coefficients in order to obtain a result. Therefore, in this study only the $A_1(k)$ coefficient is analyzed. The feature that is statistically analyzed is the difference between the auto-regressive coefficients of a known undamaged state $A_1^u(k)$ and the coefficients from a state that is to be determined $A_1^d(k)$. Damage in the structure causes the auto-regressive coefficients to differ from the undamaged coefficients for various frequencies. Certain frequencies are more sensitive to damage in the joint and cause a greater difference between auto-regressive coefficients than other frequencies. Therefore, the extracted feature will be at a maximum (or a minimum) at these certain frequencies. This result shows that the most useful data for identifying damage to the structure will come in the tails of the feature distribution.

If this new coefficient difference feature, which will now be referred to as G(k), has a Gaussian distribution, then a standard control chart (Sohn et al., 2000) could be applied to monitor the status of the system. However, by plotting the features on a normal probability chart, shown in Figure 3, it is revealed that the tails of the distribution deviate widely from that of the normal distribution; if the data were normally distributed, they would plot as a straight line. This normal probability chart clearly indicates that the data are not normally distributed and, therefore, any control chart based on the normality assumption of the data will show an inflated number of outliers for a given confidence limit, which can lead to false-positive indication of damage. The outliers will be a result of the tails of the actual distribution being much longer than that of the normal distribution. This result can be seen in Figure 4. The non-Gaussian nature of the data suggests that a different method of statistical analysis should be used.

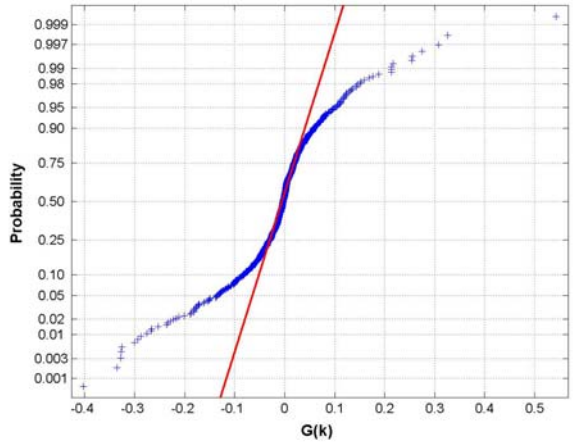

Figure 3: Normal probability plot of the feature G(k)

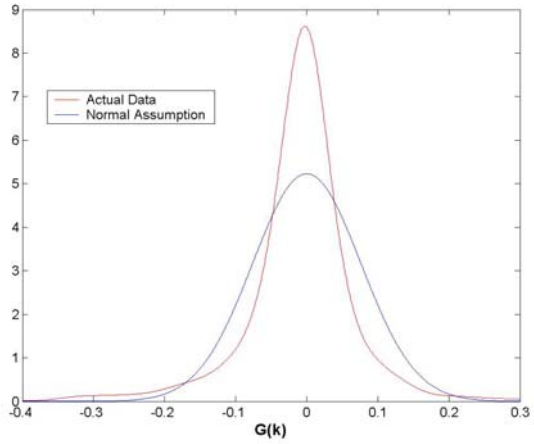

Figure 4: Probability density function of the extracted feature G(k) vs. the normality assumption

EVS is used in this analysis to accurately model the behavior of the feature distribution's tails. The basis of this branch of statistics stems from the following situation (Castillo, 1988). If a moving window is taken along a vector of samples and the maximum value is selected from each of these windows, the induced cumulative density function of the maxima of the samples, as the number of vector samples tends to infinity, converges to one of three possible distributions: Gumbel, Weibull, or Frechet.

$$\text{Gumbel: } F(x) = \exp\left[-\exp\left(\frac{\delta}{x-\lambda}\right)\right] \quad \begin{matrix} -\infty < x < \infty \\ \delta > 0 \end{matrix} \tag{2}$$

$$\text{Weibull: } F(x) = \begin{cases} 1 & \text{If } x \geq \lambda \\ \exp\left[-\left(\frac{\delta}{x-\lambda}\right)^{\beta}\right] & \text{otherwise} \end{cases} \tag{3}$$

$$\text{Frechet: } F(x) = \begin{cases} \exp\left[-\left(\frac{\delta}{x-\lambda}\right)^{\beta}\right] & \text{If } x \geq \lambda \\ 0 & \text{otherwise} \end{cases} \tag{4}$$

where λ, δ and β are the model parameters that are estimated from the data. Similarly, there are only three different types of distributions for minima.

The appropriate distribution is then chosen by plotting the extracted vector of maxima on the probability paper for a Gumbel distribution. The vector will plot in a linear fashion if it has a Gumbel maximum distribution. Otherwise, the vector will have an associated curvature. If this curvature is concave, the feature vector has a Weibull maximum distribution. Similarly, if the curvature is convex, the feature vector has a Frechet maximum distribution. A parametric model is then fit using the chosen distribution and produces the model parameters. For the Frechet and Weibull distributions, the location parameter λ must be estimated *a priori* to computing the running the δ and β parameters. While there are a few statistical manners by which to choose this parameter, in this study it was chosen by using an initial guess based on the parameter's limits and then choosing the final value by observing the plot of the analytical model along with the actual vector of data.

Once the model parameters are chosen, it is possible to generate true confidence limits that can be applied to the distribution. These limits are far more accurate than those obtained when assuming a simple Gaussian distribution. The threshold corresponding to a specific confidence level are given by the following equations:

$$\text{Gumbel: } x_{max} = \lambda - \delta \ln\left[-\ln\left(1-\frac{n\alpha}{2}\right)\right] \tag{5}$$

$$\text{Weibull: } x_{max} = \lambda - \delta \ln\left[-\ln\left(1-\frac{n\alpha}{2}\right)\right]^{\frac{1}{\beta}} \tag{6}$$

$$\text{Frechet: } x_{max} = \lambda + \frac{\delta}{\left[-\ln\left(1-\frac{n\alpha}{2}\right)\right]^{\frac{1}{\beta}}} \tag{7}$$

where n is the window size used to extract the maxima and α is the associated Type I error of the confidence limit. It should be noted that the upper confidence limit is calculated from the associated maxima distribution and the lower confidence limit is calculated from the associated minima distribution. For simplicity, only the maxima distribution and upper confidence limit are mentioned in the analysis procedure. However, minima distribution and the lower confidence limit can be readily found in a similar manner.

In this study, the original length of the time signal is 4096 points. Using blocks of 2048 with 75% overlap reduces the sample length to 2048. Applying the FFT to each block further reduces the sample length to 1024 points in the frequency domain. Of these points, only the first 800 points are used, to disregard the effect of a leakage problem at the high frequency range. Therefore, the parent distribution of G(k) has 800 data points. A window of 10 samples is moved along

the parent vector and the maximum of each window is then extracted. This process generates a maxima vector of 80 points to be analyzed by EVS. Once a distribution is chosen, the model parameters must be estimated. Only a portion of the data points in the maxima vector are used to compare to the fitted model, because agreement with the upper and lower ends of the extracted maxima vector is more important than agreement with the entire vector. An example of this result can be seen in Figure 5, which shows an accepted fit of maxima in a Frechet distribution.

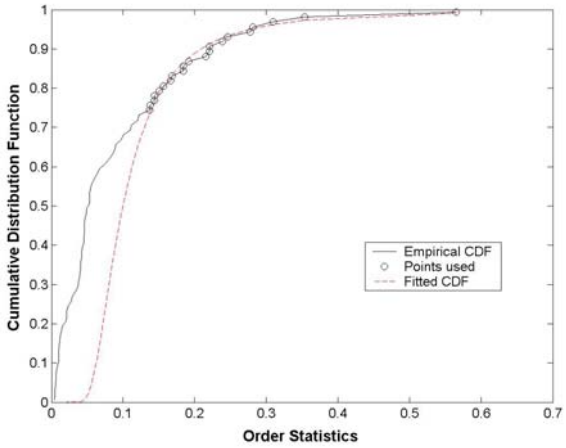

Figure 5: Curve fit for Frechet maxima distribution

Once a model has been fit for both the maxima and minima of a parent distribution, the confidence limits are calculated using the previous equations for the threshold values. In this study, confidence levels of 99%, 99.5%, and 99.9% were tested to see which gave the best results. It was determined that a confidence level of 99.5% ($\alpha = 0.005$) was best suited to the data used in this analysis.

4. EXPERIMENTAL RESULTS

Five sets of data are used in each analysis. The first set is the baseline undamaged data that are used to set the confidence limits. These limits are tested against data sets from all three damage levels (15 in-lb, 5 in-lb, and no bolts) and against another undamaged case to be sure that false positives are not a problem. For all cases, it was determined that the Frechet distribution, for either maxima or minima, was the most appropriate extreme value distribution to use for the analysis. After the location parameter, λ, is estimated through trial-and-error, the other model parameters are found by fitting the parametric model to the extracted maximum and minimum data. The upper and lower confidence limits corresponding to a 99.5% confidence interval are then calculated from the known parameters using Equation (7), or an equivalent equation for minima. For a sample size of 800 points and a 99.5% confidence interval, one should expect 2 outliers on each side of the confidence interval.

Previous work has shown that the application of the EVS-based statistical model shows excellent results when applied to a joint in the structure that is known to be damaged (Fasel et al., 2003). Table 2 illustrates the effectiveness of the limits found using EVS versus those calculated using the normality assumption of the data. All numbers displayed in parentheses are associated with the normality assumption.

Table 2: Number of outliers for particular damage case at the damaged joint

	Lower outliers	Upper outliers
Baseline	1 (15)	1 (10)
15 in-lb torque	88 (166)	20 (64)
5 in-lb torque	110 (202)	20 (64)
Bolt removed	9 (30)	38 (111)
Undamaged	2 (11)	0 (12)

* Results from the normality assumption are shown in parentheses.

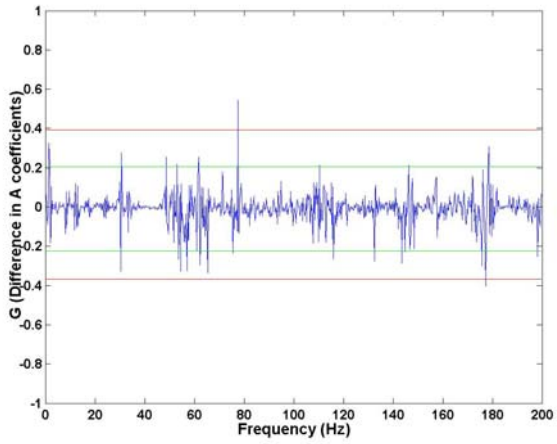

Figure 6: 99.5% Confidence Interval of baseline undamaged case with legend (solid line: G(*k*), solid outer line: EVS confidence limit, dashed inner line: normal confidence limit)

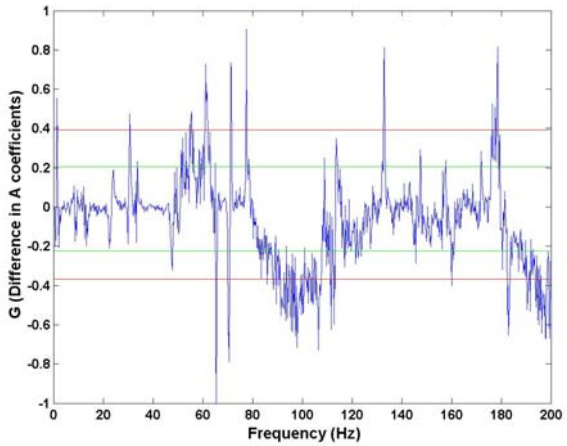

Figure 7: 99.5% Confidence Interval of 15 in-lb damage case with legend (solid line: G(*k*), solid outer line: EVS confidence limit, dashed inner line: normal confidence limit)

Clearly, the confidence limits derived using EVS is much closer to the actual 99.5% limits than those derived using the normality assumption. This result can also be expressed graphically. Figures 6 and 7 show plots of data and confidence limits for the baseline undamaged case and the 15 in-lb damage case.

Figure 6 shows only one outlier on each side of the confidence interval. That result is slightly less than the expected outcome of two outliers on each side, but does not produce a false positive result so it is acceptable. It is clear that if confidence limits based upon the normality assumption are used, there are many false positives, which negates any usefulness that the analysis method sought.

Figure 7 shows the effectiveness of using coefficients from the frequency domain ARX model. There is a clear graphical aberration from the data taken during the undamaged state. Both the EVS and normal confidence limits correctly indicate damage has taken place. However, the EVS confidence limits show the frequency range in which the accelerometer response is truly affected by the damage in the system.

Several damage cases were fully analyzed by examining data from each of the 12 joints on the test structure that are instrumented with accelerometers. The focus of this study is the application of the aforementioned damage detection scheme to undamaged joints in the test structure. Results from two damage cases that best show the effectiveness of this method are shown here.

The first set of data comes from a damage case in which joint 2a, which is on the corner farthest from the shaker on third (highest) floor of the test structure, was the damaged joint. In this case, the structure was excited at its base at the high level (1 V) done for this experiment. The results of the aforementioned damage detection scheme can be seen in Table 3. Again, the expected number of outliers for an undamaged joint is 4 when the confidence limits are established using EVS. Results from the undamaged test case are mostly positive, with only 1 joint out of 12 showing a false positive indication of damage. While the method appears to have failed due to the large number of outliers, a graphical inspection of the test feature G(*k*) along with the EVS confidence limits shows that 5 of the outliers are just beyond the established confidence limit. Such results would be less likely to occur with a larger amount of baseline data to establish the EVS confidence limits; the results would also benefit from a more rigorous optimization protocol for choosing the EVS parameters. Currently the location parameter is established only through a trial and error procedure.

Table 3: Total number of outliers using EVS confidence limits for particular damage cases under the high level (1 V) of base excitation. The shaded region indicates the damaged joint in the structure.

	Joints											
	1st Floor				2nd Floor				3rd Floor			
	1	2	3	4	5	6	7	8	9	10	11	12
Undamaged	9	4	3	2	2	4	4	2	2	2	3	3
15 in-lb damage	16	27	38	18	15	12	18	15	32	58	35	22
5 in-lb damage	25	30	38	17	16	16	19	16	40	90	31	23
No bolt damage	34	28	37	23	24	17	21	28	39	25	33	24

The damage cases, however, show that the damage detection scheme is unable to localize damage and causes all joints in the test structure to appear damaged according to the number of outliers. For the cases in which the bolts are loosened, but not removed, from the structure, the joint at which the damage was induced showed the largest number of outliers. This would seem to indicate that the actual damage might be able to be localized using this method. However, for cases in which multiple joints in the building are damaged, choosing the joint with the highest number of outliers as the only damaged joint would not produce a correct result. In addition, in examining the damage case in which the bolt is completely removed, it can be seen that many other joints in the building actually produce more outliers than the damaged joint does. This is most likely because the damage detection scheme is based on the modeling of the nonlinear system input/output relationship. When the bolt is completely removed, the source of local nonlinearity (the loose bolt rattling against the plate) disappeared. This causes the number of outliers detected using the EVS confidence limits to drastically drop when compared to the other damage cases.

The second set of data comes from a damage case in which joint 4b, which is on the corner directly above the shaker on the second (middle) floor of the test structure, was the damaged joint. In this case, the structure was being excited at its base at the low level (0.25 V) of excitation. The results can be seen in Table 4. Again, the expected number of outliers for an undamaged joint is 4 when the confidence limits are established using EVS. The undamaged test case shows somewhat worse results than in the first case. This result is backed up when looking at the test feature along with the EVS confidence limits in a graphical manner. It is seen that the low level of excitation tends to produce more extreme data than the high level of excitation. The level of excitation is likely not high enough to fully differentiate the accelerometer response due to the base excitation and the response due to ambient background noise. Therefore, it is concluded that the lower excitation level tends to be more sensitive to false positive results than the higher excitation level. This outcome demonstrates the need for a different normalization procedure, as normalizing the time data should result in similar results for different levels of base excitation to the structure.

Table 4: Total number of outliers using EVS confidence limits for particular damage cases under the low level (0.25 V) of base excitation. The shaded region indicates the damaged joint in the structure.

	Joints											
	1st Floor				2nd Floor				3rd Floor			
	1	2	3	4	5	6	7	8	9	10	11	12
Undamaged	3	6	4	3	9	3	4	4	4	8	10	4
15 in-lb damage	13	14	24	31	24	40	22	24	28	19	29	21
5 in-lb damage	11	15	31	33	23	39	25	22	32	20	27	18
No bolt damage	18	15	28	29	42	53	27	35	40	25	44	33

Examination of the damage cases leads to more of the same conclusions. The results are not as good as with the high excitation, as the numbers of outliers from the damaged joint are never the highest of all joints. The low number of outliers for the damage cases involving the bolt still being present is most likely due to the inability of the low input level to excite the nonlinearity in the damaged joint. The inability of the current method to localize damage within the structure indicates that a new method must be undertaken to address this vulnerability.

5. PATH FORWARD

In recent years, an impedance-based method using PZT patches as both actuators and sensors has been proven a very powerful tool in structural health monitoring. A voltage is applied to a PZT patch that has been bonded to the structure. This voltage exerts a force in the local area of the PZT patch. This force then induces a stress in the structure that causes the current output of the PZT patch to change (See Figure 8). The electrical impedance (V/I) calculated in this manner can be shown to be directly related to the structural impedance. The impedance-based method is shown to be excellent at localizing damage because input to the structure is generally greater than 30 kHz. For more information on current impedance-based SHM methods, consult Park et al., 2000. To date, impedance based methods have focused on using the real part of the induced electrical impedance as the extracted feature for use in SHM. The author proposes to use the voltage into the PZT as the input to the frequency domain ARX model and the current as the output. Only the real part of the information would be used due to the extreme temperature sensitivity of the imaginary part of the data. Again, the difference in A coefficients determined by the ARX model would be used, along with EVS, to determine the damage state of each joint. The use of EVS with the impedance-based method is important because there are currently no limits framed in a rigorous statistical manner that have been used with this method. The use of the impedance method has great potential to solve previously stated problems with data normalization and damage localization in the current frequency domain ARX method.

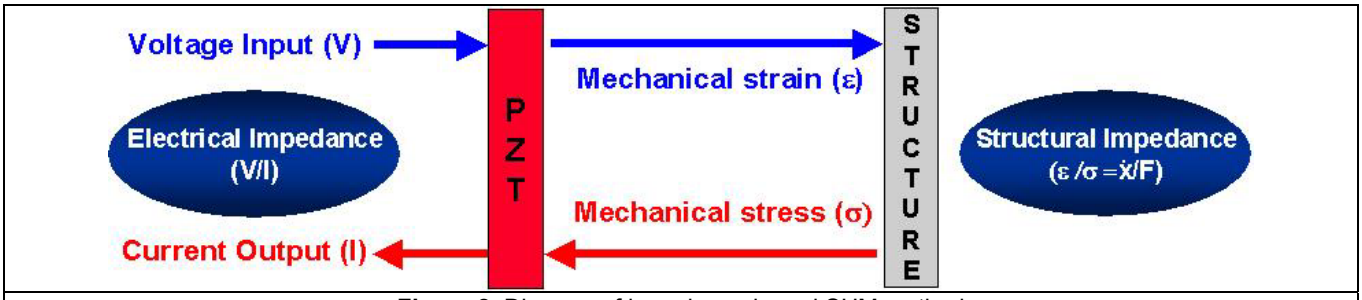

Figure 8: Diagram of impedance-based SHM method

6. SUMMARY

Coefficients from a frequency domain ARX model show promise as a powerful feature for damage discrimination. The addition of EVS as a means for establishing true confidence limits greatly enhances this damage classification technique. Unfortunately, the current method is unable to localize damage in a test structure to a particular joint. The path forward involves the integration of the promising impedance-based method into the frequency domain ARX model. It is hoped that the ability of the ARX model to examine nonlinearities within the structure as well as the rigorous statistical boundaries found through the application of EVS will result in a damage detection scheme that is able to localize damage within the structure without producing any false positive results.

ACKNOWLEDGEMENT

Funding for this project was provided by the Department of Energy through the internal funding program at Los Alamos National Laboratory known as Laboratory Directed Research and Development. The author acknowledges Tim Johnson and Seth Gregg and the Los Alamos Dynamic Summer School for providing the test structure as well as helping with the set-up, instrumentation and acquisition of data from the test structure. Funding for the summer school was provided by the Engineering Sciences and Application Division at Los Alamos National Laboratory and the Department of Energy's Education Program Office.

REFERENCES

1. Doebling, S.W., Farrar, C.R. and Prime, M.B., "A Summary Review of Vibration-Based Damage Identification Methods," *The Shock and Vibration Digest*, **30**(2), pp. 91-105, 1998.

2. Farrar, C.R., Doebling, S.W., Nix, D.A., "Vibration-Based Structural Damage Identification," *Philosophical Transactions of the Royal Society: Mathematical, Physical & Engineering Sciences*, **359**(1778), pp. 131-149, 2001.

3. Adams, D.E. and Allemang, R.J., "Discrete Frequency Models: A New Approach to Temporal Analysis," *ASME Journal of Vibration and Acoustic*, **123**, pp. 98-103, 2000.

4. Adams, D.E., "Frequency Domain ARX Models and Multi-Harmonic FRF Estimators for Nonlinear Dynamic Systems," *Journal of Sound and Vibration*, **250**(5), pp. 935-950, 2001.

5. Sohn, H., Czarnecki, J.J. and Farrar, C.R., "Structural Health Monitoring Using Statistical Process Control," *Journal of Structural Engineering*, **126**(11), pp. 1356-1363, 2000.

6. Castillo, E., *Extreme Value Theory in Engineering*, Academic Press Series in Statistical Modeling and Decision Science, San Diego, CA, 1988.

7. Fasel, T.R., Sohn, H. and Farrar, C.R., "Damage Detection Using Frequency Domain ARX Models and Extreme Value Statistics," *The 21st International Modal Analysis Conference*, Kissimmee, FL, USA, February 3-6, 2003.

8. Park, G., Cudney, H. and Inman, D.J., "Impedance-Based Health Monitoring of Civil Structural Components," *Journal of Infrastructure Systems*, **6**(4), pp. 153-160, 2000.